




# Mononuclear five-coordinate cobalt(II) complexes with N<sub>4</sub>-coordinate pyrazole based ligand and pseudohalogens: synthesis, structures, DNA and protein binding study

Ankita Solanki, Yogesh Prakash Patil & Sujit Baran Kumar


To cite this article: Ankita Solanki, Yogesh Prakash Patil & Sujit Baran Kumar (2015) Mononuclear five-coordinate cobalt(II) complexes with N<sub>4</sub>-coordinate pyrazole based ligand and pseudohalogens: synthesis, structures, DNA and protein binding study, Journal of Coordination Chemistry, 68:22, 4017-4037, DOI: [10.1080/00958972.2015.1085515](https://doi.org/10.1080/00958972.2015.1085515)



To link to this article: <http://dx.doi.org/10.1080/00958972.2015.1085515>

 View supplementary material 

 Accepted author version posted online: 25 Aug 2015.  
Published online: 21 Sep 2015.

 Submit your article to this journal 

 Article views: 108

 View related articles 

 View Crossmark data 

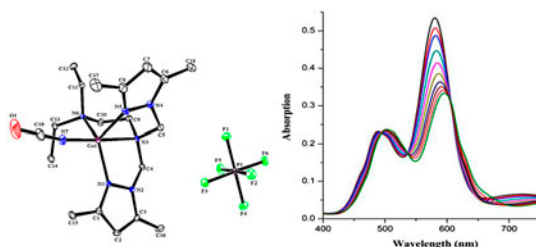
# Mononuclear five-coordinate cobalt(II) complexes with N<sub>4</sub>-coordinate pyrazole based ligand and pseudohalogen: synthesis, structures, DNA and protein binding study

ANKITA SOLANKI<sup>†</sup>, YOGESH PRAKASH PATIL<sup>‡</sup> and SUJIT BARAN KUMAR<sup>\*†</sup>

<sup>†</sup>Faculty of Science, Department of Chemistry, The Maharaja Sayajirao University of Baroda, Vadodara, India

<sup>‡</sup>Inorganic and Physical Chemistry Department, Indian Institute of Science, Bangalore, India

(Received 8 August 2014; accepted 6 August 2015)



A series of mononuclear five-coordinate cobalt(II) complexes, [Co(X)(dbdmp)]Y, where dbdmp = *N,N*-diethyl-*N,N'*-bis((3,5-dimethyl-1*H*-pyrazol-1-yl)methyl)ethane-1,2-diamine, X = N<sub>3</sub><sup>-</sup>/NCO<sup>-</sup>/NCS<sup>-</sup> and Y = PF<sub>6</sub><sup>-</sup>/BF<sub>4</sub><sup>-</sup>/ClO<sub>4</sub><sup>-</sup>, have been synthesized and characterized by microanalyses and spectroscopic techniques. Crystal structures of [Co(N<sub>3</sub>)(dbdmp)]PF<sub>6</sub> (**1**), [Co(N<sub>3</sub>)(dbdmp)]ClO<sub>4</sub> (**3**), [Co(NCO)(dbdmp)]PF<sub>6</sub> (**4**), [Co(NCO)(dbdmp)]ClO<sub>4</sub> (**6**), and [Co(NCS)(dbdmp)]ClO<sub>4</sub> (**9**) have been solved by single-crystal X-ray diffraction studies and showed that all the complexes have distorted trigonal bipyramidal geometry; PF<sub>6</sub><sup>-</sup> counter anion containing complexes [Co(N<sub>3</sub>)(dbdmp)]PF<sub>6</sub> and [Co(NCO)(dbdmp)]PF<sub>6</sub> have chiral space groups. The binding ability of synthesized complexes with CT-DNA and bovine serum albumin (BSA) has been studied by spectroscopic methods and viscosity measurements. The experimental results of absorption titration of cobalt(II) complexes with CT-DNA indicate that the complexes have ability to form adducts and they can stabilize the DNA helix. The cobalt(II) complexes exhibit good binding propensity to BSA protein.

**Keywords:** Tetradentate ligand; Cobalt(II); Pseudohalides; Structures; DNA; BSA binding

## 1. Introduction

Syntheses of new transition metal complexes as anticancer agents constitute an important area of research. Transition metal complexes have been used to study interactions with DNA because of their versatile coordination, redox, and structural properties. DNA is also a

\*Corresponding author. Email: [sujit\\_baran@yahoo.com](mailto:sujit_baran@yahoo.com)

good target for metal complexes because of its wide variety of binding sites [1–4]. Cobalt is an essential element in the biological system and it regulates the synthesis of DNA indirectly as it is an active center of vitamin B12. The interaction of DNA with cobalt complexes with nitrogen-based ligands has attracted much attention [5, 6]. There are many reports on the interaction of DNA with copper(II) complexes but there are few reports on DNA binding with cobalt(II) [7–12] and cobalt(III) complexes [13–17] based on nitrogen and oxygen containing ligands.

Nitrogen-containing heterocyclic compounds like imidazole or pyrazole play an important role in biological systems. We have reported syntheses, structures, and DNA binding study of copper(II) complexes with pseudohalogens and pyrazole-containing tripodal ligand, and the results show such complexes have strong interaction with DNA [18]. Although pseudohalides are ambidentate, we obtain mononuclear cobalt(II) complexes, like copper(II) complexes, in the presence of pyrazole-containing tripodal ligand and pseudohalides such as azide, thiocyanate, or isocyanate. The objective of the work was to see whether cobalt(II) complexes with the same ligand and pseudohalides have any interaction with DNA and bovine serum albumin (BSA).

We report syntheses, characterizations, and X-ray crystal structures of mononuclear cobalt(II) complexes,  $[\text{Co}(\text{X})(\text{dbdmp})]\text{Y}$ , where  $\text{dbdmp} = N,N$ -diethyl- $N',N'$ -bis((3,5-dimethyl-1*H*-pyrazol-1-yl)methyl)ethane-1,2-diamine, a tetradentate  $\text{N}_4$ -coordinated ligand,  $\text{X} = \text{N}_3^-/\text{NCO}^-/\text{NCS}^-$  and  $\text{Y} = \text{PF}_6^-/\text{BF}_4^-/\text{ClO}_4^-$ . Crystal structures of  $[\text{Co}(\text{N}_3)(\text{dbdmp})]\text{PF}_6$  (**1**),  $[\text{Co}(\text{N}_3)(\text{dbdmp})]\text{ClO}_4$  (**3**),  $[\text{Co}(\text{NCO})(\text{dbdmp})]\text{PF}_6$  (**4**),  $[\text{Co}(\text{NCO})(\text{dbdmp})]\text{ClO}_4$  (**6**), and  $[\text{Co}(\text{NCS})(\text{dbdmp})]\text{ClO}_4$  (**9**) have been solved by single-crystal X-ray diffraction studies and show that all the complexes have distorted trigonal bipyramidal geometry. DNA binding of the complexes was explored by absorption and fluorescence spectroscopy and protein (BSA) binding by fluorescence spectroscopy. The interaction of CT-DNA with cobalt(II) complexes by absorption spectroscopy shows several isobestic points, indicating the formation of new complexes with DNA and cobalt(II).

## 2. Experimental

### 2.1. Materials

The chemicals and solvents were of analytical grade and purchased from commercial sources. Acetylacetone, paraformaldehyde, hydrazine hydrate, sodium azide, sodium isocyanate, potassium thiocyanate,  $\text{Co}(\text{CH}_3\text{COO})_2 \cdot 4\text{H}_2\text{O}$  (Qualigens, India),  $N,N$ -diethylethylenediamine,  $\text{NH}_4\text{PF}_6$ ,  $\text{NH}_4\text{BF}_4$  (Aldrich), calf thymus-DNA (CT-DNA), ethidium bromide, BSA, tris(hydroxymethyl)aminomethane hydrochloride (Tris-HCl), and NaCl (Spectrochem, India) were of reagent grade and used as received.  $N,N$ -diethyl- $N',N'$ -bis((3,5-dimethyl-1*H*-pyrazol-1-yl)methyl)ethane-1,2-diamine (dbdmp) was synthesized according to the reported method [18].  $\text{Co}(\text{ClO}_4)_2 \cdot 6\text{H}_2\text{O}$  was prepared by reaction of cobalt carbonate with dilute  $\text{HClO}_4$  acid and followed by slow evaporation of the solution.

### 2.2. Synthesis of complexes

*Caution!* Transition metal complexes with perchlorate, azide ion, and organic ligands are potentially explosive. Only a small amount of material should be synthesized, and it should be handled with care.

**2.2.1. [Co(N<sub>3</sub>)(dbdmp)]X, X = PF<sub>6</sub><sup>-</sup> (1) and BF<sub>4</sub><sup>-</sup> (2).** A methanol solution (10 mL) of dbdmp (0.166 g, 0.5 mmol) was added dropwise to a stirring solution of Co(CH<sub>3</sub>COO)<sub>2</sub>·4H<sub>2</sub>O (0.125 g, 0.5 mmol) in the same solvent (10 mL). To this solution, NaN<sub>3</sub> (0.032 g, 0.5 mmol) in water (0.5 mL) was added slowly. After 10 min, NH<sub>4</sub>PF<sub>6</sub>/NH<sub>4</sub>BF<sub>4</sub> (0.5 mmol) in water (1 mL) was added and the blue solution was stirred for 4–5 h, filtered and kept at room temperature for slow evaporation. Plate-shaped dark brown X-ray quality single crystals were obtained after seven days.

[Co(N<sub>3</sub>)(dbdmp)]PF<sub>6</sub> (1). Yield 0.120 g (41%). Found: C = 37.25, H = 5.59, N = 21.96%, Anal. Calcd for C<sub>18</sub>H<sub>32</sub>N<sub>9</sub>PF<sub>6</sub>Co: C = 37.38, H = 5.58, N = 21.79%. IR (KBr pellet) cm<sup>-1</sup>; ν(N<sub>3</sub><sup>-</sup>), 2072 vs; ν(C=C) + ν(C=N) (pz) ring, 1554 s, 1467 s; ν(PF<sub>6</sub><sup>-</sup>), 845. UV–vis spectra: λ<sub>max</sub>(CH<sub>3</sub>CN) (nm) (ε<sub>max</sub> (mol<sup>-1</sup> cm<sup>-1</sup>)). 781 (30), 606 (232), 502 (109), 332 (1099), 249 (3698). Λ<sub>M</sub>(CH<sub>3</sub>CN)(Ω<sup>-1</sup> cm<sup>2</sup> mol<sup>-1</sup>) = 122. μ<sub>eff</sub> = 4.27 BM.

[Co(N<sub>3</sub>)(dbdmp)]BF<sub>4</sub> (2). Yield 0.155 g (60%). Found: C = 41.75, H = 6.19, N = 24.76%, Anal. Calcd for C<sub>18</sub>H<sub>32</sub>N<sub>9</sub>BF<sub>4</sub>Co: C = 41.56, H = 6.20, N = 24.23%. IR (KBr pellet) cm<sup>-1</sup>; ν(N<sub>3</sub><sup>-</sup>), 2065 vs; ν(C=C) + ν(C=N) (pz) ring, 1551 s, 1466 s; ν(BF<sub>4</sub><sup>-</sup>), 1028–1068(br). UV–vis spectra: λ<sub>max</sub>(CH<sub>3</sub>CN) (nm) (ε<sub>max</sub> (mol<sup>-1</sup> cm<sup>-1</sup>)). 780 (39), 606 (305), 502 (147), 332 (1409), 243 (3652). Λ<sub>M</sub>(CH<sub>3</sub>CN)(Ω<sup>-1</sup> cm<sup>2</sup> mol<sup>-1</sup>) = 120. μ<sub>eff</sub> = 4.16 BM.

**2.2.2. [Co(N<sub>3</sub>)(dbdmp)]ClO<sub>4</sub> (3).** A methanol solution (10 mL) of dbdmp (0.166 g, 0.5 mmol) was added dropwise to a stirring Co(ClO<sub>4</sub>)<sub>2</sub>·6H<sub>2</sub>O (0.182 g, 0.5 mmol) solution (10 mL) in the same solvent. To this solution, NaN<sub>3</sub> (0.032 g, 0.5 mmol) in water (1 mL) was added slowly and the blue mixture was stirred for 4–5 h, filtered, and kept at room temperature for slow evaporation. Blue single crystals were collected after 5 days. Yield 0.140 g (41%). Found: C = 40.55, H = 5.99, N = 23.43%, Anal. Calcd for C<sub>18</sub>H<sub>32</sub>N<sub>9</sub>ClO<sub>4</sub>Co: C = 40.57, H = 6.05, N = 23.66%. IR (KBr pellet) cm<sup>-1</sup>; ν(N<sub>3</sub><sup>-</sup>), 2067 vs; ν(C=C) + ν(C=N) (pz) ring, 1549 s, 1558 s, 1463 s; ν<sub>asym</sub>(Cl–O), 1078; δ(O–Cl–O), 624 s. UV–vis spectra: λ<sub>max</sub>(CH<sub>3</sub>CN) (nm) (ε<sub>max</sub> (mol<sup>-1</sup> cm<sup>-1</sup>)). 778 (33), 606 (276), 502 (128), 332 (1288), 242 (3741). Λ<sub>M</sub>(CH<sub>3</sub>CN)(Ω<sup>-1</sup> cm<sup>2</sup> mol<sup>-1</sup>) = 118. μ<sub>eff</sub> = 4.24 BM.

**2.2.3. [Co(NCO)(dbdmp)]PF<sub>6</sub> (4).** To a stirring solution of Co(CH<sub>3</sub>COO)<sub>2</sub>·4H<sub>2</sub>O (0.125 g, 0.5 mmol) in methanol (10 mL), dbdmp (0.166 g, 0.5 mmol) in methanol was added dropwise. After 10 min, NaNCO (0.032 g, 0.5 mmol) in water (0.5 mL) was added. Finally, NH<sub>4</sub>PF<sub>6</sub> (0.082 g, 0.5 mmol) in water (0.5 mL) was added to the solution. This blue mixture was stirred for 3–4 h, filtered, and kept for slow evaporation. Plate-shaped dark blue X-ray quality single crystals were obtained after seven days. (Yield 0.139 g, 48%). Found: C = 39.57, H = 5.59, N = 16.90%, Anal. Calcd for C<sub>19</sub>H<sub>32</sub>N<sub>7</sub>OPF<sub>6</sub>Co: C = 39.45, H = 5.58, N = 16.95%. IR (KBr pellet) cm<sup>-1</sup>; ν(NCO<sup>-</sup>), 2229 vs; ν(C=C) + ν(C=N) (pz) ring, 1553 s, 1466 s; ν(PF<sub>6</sub><sup>-</sup>), 845. UV–vis spectra: λ<sub>max</sub>(CH<sub>3</sub>CN) (nm) (ε<sub>max</sub> (mol<sup>-1</sup> cm<sup>-1</sup>)). 765 (34), 599 (195), 489 (138), 243 (3461). Λ<sub>M</sub> (Ω<sup>-1</sup> cm<sup>2</sup> mol<sup>-1</sup>) = 116. μ<sub>eff</sub> = 4.19 BM.

**2.2.4. [Co(NCO)(dbdmp)]BF<sub>4</sub> (5).** This complex was prepared by following the same procedure as for 2 except NH<sub>4</sub>BF<sub>4</sub> was used in place of NH<sub>4</sub>PF<sub>6</sub>. Dark blue crystals were obtained. Yield 0.167 g (64%). Found: C = 43.97, H = 6.13, N = 18.96%, Anal. Calcd for C<sub>19</sub>H<sub>32</sub>N<sub>7</sub>OBF<sub>4</sub>Co: C = 43.86, H = 6.20, N = 18.85%. IR (KBr pellet) cm<sup>-1</sup>; ν(NCO<sup>-</sup>),

2214 vs;  $\nu(\text{C}=\text{C}) + \nu(\text{C}=\text{N})$  (pz) ring, 1553 s, 1466 s;  $\nu(\text{BF}_4^-)$ , 1030, 1068 b. UV-vis spectra:  $\lambda_{\text{max}}$  ( $\text{CH}_3\text{CN}$ ) (nm) ( $\epsilon_{\text{max}}$  ( $\text{mol}^{-1} \text{cm}^{-1}$ )). 766 (41), 599 (230), 489 (158), 245 (3448).  $\Lambda_{\text{M}}$  ( $\text{CH}_3\text{CN}$ )( $\Omega^{-1} \text{cm}^2 \text{mol}^{-1}$ ) = 116.  $\mu_{\text{eff}} = 4.31 \text{ BM}$ .

**2.2.5. [Co(NCO)(dbdmp)]ClO<sub>4</sub> (6).** This complex was prepared by following the same procedure as for **3** except  $\text{NaNCO}$  was used in place of  $\text{NaN}_3$ . Dark blue crystals were obtained after one week. Yield 0.150 g (58%). Found: C = 42.87, H = 6.11, N = 18.61%, Anal. Calcd for  $\text{C}_{19}\text{H}_{32}\text{N}_7\text{O}_5\text{ClCo}$ : C = 42.82, H = 6.05, N = 18.40%. IR (KBr pellet)  $\text{cm}^{-1}$ ;  $\nu(\text{NCO}^-)$ , 2218 vs;  $\nu(\text{C}=\text{C}) + \nu(\text{C}=\text{N})$  (pz) ring, 1553 s, 1466 s;  $\nu_{\text{asym}}(\text{Cl}-\text{O})$ , 1076;  $\delta(\text{O}-\text{Cl}-\text{O})$ , 624 s. UV-vis spectra:  $\lambda_{\text{max}}$ ( $\text{CH}_3\text{CN}$ ) (nm) ( $\epsilon_{\text{max}}$  ( $\text{mol}^{-1} \text{cm}^{-1}$ )). 772 (39), 599 (237), 489 (154), 245 (3517), 228 (3473).  $\Lambda_{\text{M}}$  ( $\Omega^{-1} \text{cm}^2 \text{mol}^{-1}$ ) = 122.  $\mu_{\text{eff}} = 4.18 \text{ BM}$ .

**2.2.6. [Co(NCS)(dbdmp)]X, X = PF<sub>6</sub><sup>-</sup> (7) and BF<sub>4</sub><sup>-</sup> (8).** These complexes were prepared by following the same procedure as for **1** except  $\text{KSCN}$  was used in place of  $\text{NaN}_3$ .

[Co(NCS)(dbdmp)]PF<sub>6</sub> (**7**). Yield 0.175 g (59%). Found: C = 38.27, H = 5.50, N = 16.36%, Anal. Calcd for  $\text{C}_{19}\text{H}_{32}\text{N}_7\text{SPF}_6\text{Co}$ : C = 38.39, H = 5.43, N = 16.49%. IR (KBr pellet)  $\text{cm}^{-1}$ ;  $\nu(\text{NCS}^-)$ , 2067 vs;  $\nu(\text{C}=\text{C}) + \nu(\text{C}=\text{N})$  (pz) ring, 1554 s, 1467 s;  $\nu(\text{PF}_6^-)$ , 846. UV-vis spectra:  $\lambda_{\text{max}}$  ( $\text{CH}_3\text{CN}$ ) (nm) ( $\epsilon_{\text{max}}$  ( $\text{mol}^{-1} \text{cm}^{-1}$ )). 723 (45), 580 (382), 489 (153), 319 (2408), 246 (3762), 218 (3567).  $\Lambda_{\text{M}}$  ( $\text{CH}_3\text{CN}$ )( $\Omega^{-1} \text{cm}^2 \text{mol}^{-1}$ ) = 119.  $\mu_{\text{eff}} = 4.22 \text{ BM}$ .

[Co(NCS)(dbdmp)]BF<sub>4</sub> (**8**). Yield 0.148 g (55%). Found: C = 42.77, H = 5.99, N = 18.06%, Anal. Calcd for  $\text{C}_{19}\text{H}_{32}\text{N}_7\text{SBF}_4\text{Co}$ : C = 42.55, H = 6.01, N = 18.28%. IR (KBr pellet)  $\text{cm}^{-1}$ ;  $\nu(\text{NCS}^-)$ , 2065 vs;  $\nu(\text{C}=\text{C}) + \nu(\text{C}=\text{N})$  (pz) ring, 1552 s, 1558 s, 1467 s;  $\nu(\text{BF}_4^-)$ , 1083. UV-vis spectra:  $\lambda_{\text{max}}$  ( $\text{CH}_3\text{CN}$ ) (nm) ( $\epsilon_{\text{max}}$  ( $\text{mol}^{-1} \text{cm}^{-1}$ )). 724 (49), 580 (407), 489 (165), 319 (2540), 249 (3845), 219 (3627).  $\Lambda_{\text{M}}$  ( $\text{CH}_3\text{CN}$ )( $\Omega^{-1} \text{cm}^2 \text{mol}^{-1}$ ) = 122.  $\mu_{\text{eff}} = 4.26 \text{ BM}$ .

**2.2.7. [Co(NCS)(dbdmp)]ClO<sub>4</sub> (9).** This complex was prepared by following the same procedure as for **3** except  $\text{KSCN}$  was used instead of  $\text{NaN}_3$ . Yield 0.165 g (64%). Found C = 41.82, H = 5.90, N = 17.75%, Anal. Calcd for  $\text{C}_{19}\text{H}_{32}\text{N}_7\text{O}_4\text{ClSCo}$ : C = 41.57, H = 5.88, N = 17.86%. IR (KBr pellet)  $\text{cm}^{-1}$ ;  $\nu(\text{NCS}^-)$ , 2066 vs;  $\nu(\text{C}=\text{C}) + \nu(\text{C}=\text{N})$  (pz) ring, 1553 s, 1466 s;  $\nu_{\text{asym}}(\text{Cl}-\text{O})$ , 1068;  $\delta(\text{O}-\text{Cl}-\text{O})$ , 624 s. UV-vis spectra:  $\lambda_{\text{max}}$  ( $\text{CH}_3\text{CN}$ ) (nm) ( $\epsilon_{\text{max}}$  ( $\text{mol}^{-1} \text{cm}^{-1}$ )). 726 (45), 580 (393), 492 (156), 318 (2453), 251 (3652), 218 (3460).  $\Lambda_{\text{M}}$  ( $\text{CH}_3\text{CN}$ )( $\Omega^{-1} \text{cm}^2 \text{mol}^{-1}$ ) = 118.  $\mu_{\text{eff}} = 4.32 \text{ BM}$ .

### 2.3. Physical measurements

IR spectra were recorded on a Perkin-Elmer FT-IR spectrometer RX1 using KBr pellets. The C, H, and N microanalyses were carried out using a Perkin-Elmer IA 2400 series elemental analyzer. UV-vis spectra (900–190 nm) were recorded on a Perkin-Elmer spectrophotometer model Lambda 35 in acetonitrile solution. Solution conductivities were measured in acetonitrile using Equip-Tronics conductivity meter (model no. EQ-660A). Room temperature magnetic susceptibilities of powder samples were measured using a Guoy balance using  $\text{Hg}[\text{Co}(\text{SCN})_4]$  as the reference.

## 2.4. DNA binding experiments

All spectral titration experiments involving interaction of the complexes with CT-DNA were performed in double-distilled buffer containing 50 mM Tris-HCl, 150 mM NaCl, and adjusted to pH 7.2 with 1 M hydrochloric acid. Stock solutions of cobalt(II) complexes were prepared in DMF. A solution of CT-DNA in buffer gave a ratio of UV absorption at 260 and 280 nm of *ca.* 1.9 : 1, indicating that the DNA was sufficiently free from protein. The DNA concentration per nucleotide was determined by absorption spectroscopy with the molar absorption coefficient  $6600 \text{ M}^{-1} \text{ cm}^{-1}$  at 260 nm [19, 20].

**2.4.1. Absorption spectroscopic studies.** The binding ability of the complexes with CT-DNA is studied by absorption spectroscopy. Absorption titration experiments were performed at constant concentration of the complexes ( $1 \times 10^{-3} \text{ M}$ ) with varying CT-DNA concentration. A control was added with equal quantity of CT-DNA to nullify the absorbance due to the CT-DNA at the measured wavelength. From the absorption titration data, the intrinsic binding constants ( $K_b$ ) of **1–6** with CT-DNA were determined using the Wolfe–Shimer equation [21]:

$$[\text{DNA}]/(\varepsilon_a - \varepsilon_f) = [\text{DNA}]/(\varepsilon_b - \varepsilon_f) + 1/K_b(\varepsilon_b - \varepsilon_f)$$

where  $\varepsilon_a$ ,  $\varepsilon_f$ , and  $\varepsilon_b$  correspond to  $A_{\text{obsd}}/[\text{Complex}]$ , the extinction coefficient for the free complex, and the extinction coefficient for the complex in fully bound form, respectively. Plot of  $[\text{DNA}]/(\varepsilon_a - \varepsilon_f)$  versus  $[\text{DNA}]$ , where  $[\text{DNA}]$  is the concentration of CT-DNA in base pairs, gives the value of  $K_b$  as the ratio of slope to intercept.

**2.4.2. Fluorescence spectroscopic studies.** Fluorescence quenching experiments were performed on a HITACHI, F-7000 fluorescence spectrophotometer at room temperature by adding complex solutions at different concentrations to the pretreated DNA-ethidium bromide complex in Tris buffer. All the samples were excited at 510 nm, and the emission was observed between 550 and 700 nm. The quenching constant was obtained using the Stern–Volmer equation [22]:

$$I_0/I = 1 + K_{sv}[Q]$$

where  $I_0$  and  $I$  are the emission intensities in the absence and presence of the complexes, respectively.  $K_{sv}$  is the linear Stern–Volmer quenching constant and  $[Q]$  is the total concentration of complexes.

**2.4.3. Viscosity measurements.** Viscosity experiments were carried out using Ostwald's capillary viscometer immersed in a thermostated water bath at  $30 \pm 0.01 \text{ }^\circ\text{C}$ , and flow time was measured using a digital stopwatch. The flow time of DNA solution was corrected by subtracting the flow time observed for the buffer solution. The viscosity of DNA solution has been measured in the presence of increasing amounts of cobalt(II) complexes. Each sample was measured three times, and an average flow time was calculated. Data were

represented as  $(\eta/\eta_0)$  versus binding ratio of cobalt(II) complex to DNA, where  $\eta$  is a viscosity of DNA in the presence of complex and  $\eta_0$  is the viscosity of DNA alone.

**2.4.4. Protein (BSA) binding experiments.** The protein binding studies have been performed by tryptophan fluorescence quenching experiments using bovine (BSA, 50  $\mu\text{M}$ , based on its molecular mass of 66,000 Da) in buffer (containing 50 mM Tris buffer and 150 mM NaCl in pure aqueous medium at pH 7.2). BSA was kept in the dark at 277 K. Double-distilled water was used throughout the experiment. The quenching of the emission intensity of tryptophan residue of BSA at 343 nm was monitored using **1**, **4**, and **7** in DMF as quenchers with increasing concentrations [23]. Fluorescence spectra were recorded from 290 to 450 nm with an excitation wavelength of 290 nm on a HITACHI, F-7000 fluorescence spectrophotometer.

## 2.5. X-ray crystallography

The crystallographic data, details of data collection, and some important features of the refinement for **1**, **3**, **4**, **6**, and **9** are given in table 1 and selected bond lengths and angles are given in table 2. Crystals of suitable size of **1**, **3**, **4**, **6**, and **9** were obtained by slow evaporation of methanol solution. For **1**, **4**, and **6** data were collected on a Bruker SMART APEX diffractometer equipped with a CCD area detector at 110, 273, and 293 K, respectively, and an Oxford X-CALIBUR-S diffractometer for **3** and **9** with Mo- $K_\alpha$  radiation ( $\lambda = 0.71073 \text{ \AA}$ ) and Cu- $K_\alpha$  radiation ( $\lambda = 1.541841 \text{ \AA}$ ) at 293 K, respectively. The data interpretations were processed with SAINT software [24] and CrysAlisPro, Agilent Technologies, Version 1.171.35.19 [25]. Empirical absorption correction was applied with SADABS software [26]. All structures were solved by direct methods using SHELXTL [27] and refined by full-matrix least squares based on  $F^2$  using SHELXL-97 [28]. All non-hydrogen atoms were refined anisotropically. The positions of the hydrogens either were located in the difference Fourier map or were introduced at calculated positions as riding on bonded atoms.

## 3. Results and discussion

### 3.1. Syntheses of the complexes

The mononuclear five-coordinate pseudohalide containing cobalt(II) complexes  $[\text{Co}(\text{X})(\text{dbdmp})]\text{Y}$  ( $\text{X} = \text{N}_3^-$ ,  $\text{NCO}^-$ ,  $\text{NCS}^-$ , and  $\text{Y} = \text{PF}_6^-$ ,  $\text{BF}_4^-$ ,  $\text{ClO}_4^-$ ) were readily synthesized through reaction of  $\text{Co}(\text{ClO}_4)_2 \cdot 6\text{H}_2\text{O}$  or  $\text{Co}(\text{CH}_3\text{COO})_2 \cdot 4\text{H}_2\text{O}$ , tetradentate  $\text{N}_4$ -coordinated ligand dbdmp, pseudohalides X ( $\text{N}_3^-/\text{NCS}^-/\text{NCO}^-$ ), and counter anion Y ( $\text{PF}_6^-/\text{BF}_4^-/\text{ClO}_4^-$ ) ions in 1 : 1 : 1 : 1 mol ratio in aqueous methanol at room temperature (scheme 1). There are only a few reports on five-coordinate cobalt(II) complexes with nitrogen coordinating ligands [29–38]. We have synthesized and structurally characterized new five-coordinate cobalt(II) complexes with trigonal bipyramidal geometry using tetradentate  $\text{N}_4$  ligand and pseudohalides. When the complexes  $[\text{Co}(\text{X})(\text{dbdmp})]\text{PF}_6$  ( $\text{X} = \text{N}_3^-$  and  $\text{NCO}^-$ ) are synthesized by reacting  $\text{Co}(\text{CH}_3\text{COO})_2 \cdot 4\text{H}_2\text{O}$ , dbdmp,  $\text{X}^-$  and  $\text{PF}_6^-$ , the complexes  $[\text{Co}(\text{N}_3)(\text{dbdmp})]\text{PF}_6$  (**1**) and  $[\text{Co}(\text{NCO})(\text{dbdmp})]\text{PF}_6$  (**4**) have chiral space groups, but when the complexes

Table 1. Crystal parameters of 1, 3, 4, 6, and 9.

Empirical formula	C <sub>36</sub> H <sub>64</sub> N <sub>18</sub> F <sub>12</sub> P <sub>2</sub> Co <sub>2</sub> (1)	C <sub>18</sub> H <sub>32</sub> CoN <sub>9</sub> ClO <sub>4</sub> (3)	C <sub>19</sub> H <sub>32</sub> CoN <sub>7</sub> F <sub>6</sub> OP (4)	C <sub>19</sub> H <sub>32</sub> CoN <sub>7</sub> ClO <sub>5</sub> (6)	C <sub>19</sub> H <sub>32</sub> CoN <sub>7</sub> ClO <sub>4</sub> S (9)
Formula weight	1156.85	532.91	578.42	532.90	548.96
Temperature (K)	110(2)	293	110(2)	296(2)	293(2)
Wavelength (Å)	0.71073	0.71073	0.71073	0.71073	1.54184
Crystal system	Monoclinic	Monoclinic	Orthorhombic	Monoclinic	Monoclinic
Space group	C2	<i>P2<sub>1</sub>/c</i>	<i>P2<sub>1</sub>2<sub>1</sub>2<sub>1</sub></i>	<i>P2<sub>1</sub>/c</i>	<i>P2<sub>1</sub>/c</i>
<i>a</i> (Å)	24.851(3)	8.6033(2)	8.2541(12)	8.874(5)	15.0296(4)
<i>b</i> (Å)	10.9025(10)	19.3515(4)	11.1622(16)	19.166(5)	12.0800(4)
<i>c</i> (Å)	20.5434(18)	14.5931(3)	27.594(4)	14.492(5)	14.4785(4)
$\alpha, \gamma$ (°)	90	90	90	90	90
$\beta$ (°)	109.596(2)	91.799(2)	90.00	93.613(5)	97.771(3)
Volume (Å <sup>3</sup> )	5243.7(9)	2428.36(9)	2542.3(6)	2459.9(17)	2604.54(13)
<i>Z</i>	4	4	4	4	4
Density (g cm <sup>-3</sup> )	1.465	1.458	1.511	1.439	1.400
Absorption coefficient (mm <sup>-1</sup> )	0.783	0.860	0.808	0.850	7.182
<i>F</i> (0 0 0)	2392	910	1196	1116	1148
$\theta$ range for data collection (°)	1.05–28.27	3.45–27.35	1.48–27.99	1.76–26.41	5.387–71.644
Index ranges	–32 ≤ <i>h</i> ≤ 31, –14 ≤ <i>k</i> ≤ 13, –27 ≤ <i>l</i> ≤ 26	–7 ≤ <i>h</i> ≤ 11, –23 ≤ <i>k</i> ≤ 24, –18 ≤ <i>l</i> ≤ 18	–10 ≤ <i>h</i> ≤ 10, –14 ≤ <i>k</i> ≤ 14, –18 ≤ <i>l</i> ≤ 18	–11 ≤ <i>h</i> ≤ 11, –23 ≤ <i>k</i> ≤ 23, –18 ≤ <i>l</i> ≤ 18	–18 ≤ <i>h</i> ≤ 17, –11 ≤ <i>k</i> ≤ 14, –17 ≤ <i>l</i> ≤ 11
Reflections collected	22,524	5148	15,094	32,354	52,247
Independent reflections	11,578 [ <i>R</i> (int) = 0.0295]	10,204 [ <i>R</i> (int) = 0.0300]	5808 [ <i>R</i> (int) = 0.0453]	5029 [ <i>R</i> (int) = 0.0227]	10,463 [ <i>R</i> (int) = 0.0363]
Max. and min. transmission	0.8719 and 0.7712	1.0000 and 0.64654	0.9382 and 0.7820	0.903 and 0.832	0.366 and 0.265
Data/restraints/parameters	11,578/1/643	5148/0/299	5808/0/322	5029/0/298	5083/0/298
Goodness of fit on <i>F</i> <sup>2</sup>	1.139	1.053	1.222	1.069	1.028
Final <i>R</i> indices [ <i>I</i> > 2σ( <i>I</i> )]	<i>R</i> 1 = 0.0505, <i>wR</i> 1 = 0.1155	<i>R</i> 1 = 0.0421, <i>w</i> <i>R</i> 1 = 0.1144	<i>R</i> 1 = 0.0633, <i>wR</i> 1 = 0.1257	<i>R</i> 1 = 0.0364, <i>wR</i> 1 = 0.1073	<i>R</i> 1 = 0.0608, <i>wR</i> 1 = 0.1518
<i>R</i> indices (all data)	<i>R</i> 2 = 0.0546, <i>wR</i> 2 = 0.1199	<i>R</i> 2 = 0.0509, <i>w</i> <i>R</i> 2 = 0.1226	<i>R</i> 2 = 0.0700, <i>wR</i> 2 = 0.1280	<i>R</i> 2 = 0.0466, <i>wR</i> 2 = 0.1242	<i>R</i> 2 = 0.0820, <i>wR</i> 2 = 0.1699
Largest diff. peak/hole (e Å <sup>-3</sup> )	0.967/–0.423	0.520/–0.296	0.806/–0.783	0.416/–0.332	0.503/–0.498
Flack parameters	0.034(11)		0.05(2)		



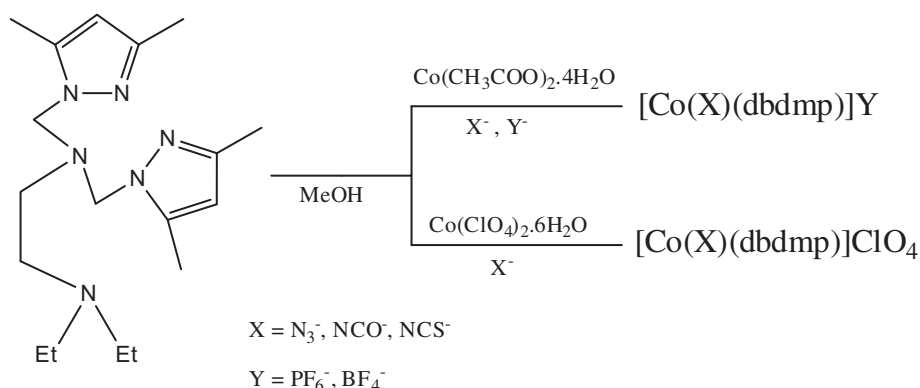
Table 2. Bond lengths (Å) and bond angles (°) of **1**, **3**, **4**, **6**, and **9**.

Bond lengths (Å)				
[Co(N <sub>3</sub> )(dbdmp)]PF <sub>6</sub>		[Co(N <sub>3</sub> )(dbdmp)]ClO <sub>4</sub>		
Co(1)–N(7)	2.001(3)	Co(2)–N(16)	1.983(3)	
Co(1)–N(1)	2.036(3)	Co(2)–N(14)	2.031(3)	
Co(1)–N(5)	2.055(3)	Co(2)–N(10)	2.039(3)	
Co(1)–N(6)	2.117(3)	Co(2)–N(15)	2.118(3)	
Co(1)–N(3)	2.256(3)	Co(2)–N(12)	2.279(3)	
[Co(NCO)(dbdmp)]PF <sub>6</sub>		[Co(NCO)(dbdmp)]ClO <sub>4</sub>		
Co(1)–N(7)	1.951(3)	Co(1)–N(7)	1.975(3)	
Co(1)–N(1)	2.039(3)	Co(1)–N(1)	2.053(2)	
Co(1)–N(5)	2.049(3)	Co(1)–N(5)	2.078(2)	
Co(1)–N(6)	2.108(3)	Co(1)–N(6)	2.130(2)	
Co(1)–N(3)	2.329(3)	Co(1)–N(3)	2.243(2)	
			Co(1)–N(7)	1.999(2)
			Co(1)–N(1)	2.067(2)
			Co(1)–N(5)	2.040(2)
			Co(1)–N(6)	2.124(2)
			Co(1)–N(3)	2.2435(19)
			N(7)–C(19)	1.149(5)
			C(19)–S(1)	1.607(4)
Bond angles (°)				
[Co(N <sub>3</sub> )(dbdmp)]PF <sub>6</sub>		[Co(N <sub>3</sub> )(dbdmp)]ClO <sub>4</sub>		
N(7)–Co(1)–N(1)	104.99(12)	N(16)–Co(2)–N(14)	104.79(13)	
N(7)–Co(1)–N(5)	102.06(13)	N(16)–Co(2)–N(10)	100.67(13)	
N(1)–Co(1)–N(5)	118.90(12)	N(14)–Co(2)–N(10)	115.65(12)	
N(7)–Co(1)–N(6)	96.14(13)	N(16)–Co(2)–N(15)	99.63(14)	
N(1)–Co(1)–N(6)	119.29(12)	N(14)–Co(2)–N(15)	120.93(12)	
N(5)–Co(1)–N(6)	110.72(12)	N(10)–Co(2)–N(15)	111.22(11)	
N(7)–Co(1)–N(3)	177.25(13)	N(16)–Co(2)–N(12)	177.63(12)	
N(1)–Co(1)–N(3)	77.45(11)	N(14)–Co(2)–N(12)	76.37(12)	
N(5)–Co(1)–N(3)	77.61(11)	N(10)–Co(2)–N(12)	76.96(11)	
N(6)–Co(1)–N(3)	81.48(12)	N(15)–Co(2)–N(12)	81.39(11)	
[Co(NCO)(dbdmp)]PF <sub>6</sub>		[Co(NCO)(dbdmp)]ClO <sub>4</sub>		
N(7)–Co(1)–N(1)	105.65(15)	N(7)–Co(1)–N(1)	104.84(9)	
N(7)–Co(1)–N(5)	102.36(15)	N(7)–Co(1)–N(5)	102.35(10)	
N(1)–Co(1)–N(5)	119.05(14)	N(1)–Co(1)–N(5)	112.73(8)	
N(7)–Co(1)–N(6)	98.50(15)	N(7)–Co(1)–N(6)	99.53(19)	
N(1)–Co(1)–N(6)	118.25(13)	N(1)–Co(1)–N(6)	109.45(7)	
N(5)–Co(1)–N(6)	109.38(14)	N(5)–Co(1)–N(6)	124.76(8)	
N(7)–Co(1)–N(3)	178.40(15)	N(7)–Co(1)–N(3)	178.13(9)	
N(1)–Co(1)–N(3)	75.90(12)	N(1)–Co(1)–N(3)	76.58(7)	
N(5)–Co(1)–N(3)	77.06(13)	N(5)–Co(1)–N(3)	73.91(7)	
N(6)–Co(1)–N(3)	80.34(12)	N(6)–Co(1)–N(3)	81.04(7)	
			N(7)–Co(1)–N(1)	104.31(10)
			N(7)–Co(1)–N(5)	106.80(9)
			N(1)–Co(1)–N(5)	112.17(8)
			N(7)–Co(1)–N(6)	95.75(9)
			N(1)–Co(1)–N(6)	124.97(8)
			N(5)–Co(1)–N(6)	109.83(8)
			N(7)–Co(1)–N(3)	176.15(9)
			N(1)–Co(1)–N(3)	75.84(8)
			N(5)–Co(1)–N(3)	76.53(7)
			N(6)–Co(1)–N(3)	81.16(7)
			[Co(NCS)(dbdmp)]ClO <sub>4</sub>	
			N(7)–Co(1)–N(1)	104.66(13)
			N(7)–Co(1)–N(5)	1024.56(14)
			N(1)–Co(1)–N(5)	113.29(12)
			N(7)–Co(1)–N(6)	95.92(13)
			N(1)–Co(1)–N(6)	122.76(11)
			N(5)–Co(1)–N(6)	111.94(12)
			N(7)–Co(1)–N(3)	175.78(13)
			N(1)–Co(1)–N(3)	76.97(10)
			N(5)–Co(1)–N(3)	78.08(11)
			N(6)–Co(1)–N(3)	79.99(10)

[Co(X)(dbdmp)]ClO<sub>4</sub> (X = N<sub>3</sub><sup>-</sup>, NCS<sup>-</sup>, NCO<sup>-</sup>) are synthesized using Co(ClO<sub>4</sub>)<sub>2</sub>·6H<sub>2</sub>O, ligand, and X<sup>-</sup>, the complexes have non-chiral space groups. Molar conductivity measurement in CH<sub>3</sub>CN solution (~10<sup>-3</sup> M) shows all the complexes are 1 : 1 electrolytes (Λ<sub>M</sub> ~ 120 Ω<sup>-1</sup> cm<sup>2</sup> mol<sup>-1</sup>) and there was no change of molar conductivity even after 2 h, indicating no dissociation of the complexes in solution. The presence of counter anion was confirmed by IR spectra and single-crystal X-ray diffraction studies. All complexes gave satisfactory microanalysis results confirming their composition. The complexes are soluble in common organic solvents like acetonitrile, methanol, ethanol, acetone, but insoluble in water.

### 3.2. Spectral and magnetic studies

The IR spectra of the complexes were assigned in comparison with spectra of the ligand. The complexes show two intense bands at ~1550 and ~1460 cm<sup>-1</sup> due to ν(C=C) + ν(C=N)



Scheme 1. Syntheses of complexes.

of pyrazole ring, and these two bands are also present in the ligand indicating coordination of dbdmp in the cobalt complexes. Complexes **1–3** exhibit a very strong band at  $\sim 2071 \text{ cm}^{-1}$  which is assigned to asymmetric stretch of N-bonded terminal  $\nu(\text{N}_3)$  band. A strong band at 2229, 2214, and  $2218 \text{ cm}^{-1}$  is assigned to N-bonded  $\text{NCO}^-$  for **4**, **5**, and **6**, respectively, and is confirmed by single-crystal X-ray crystallography [39]. A sharp peak at  $2067\text{--}2069 \text{ cm}^{-1}$  appeared for **7–9** due to N-bonded  $\nu(\text{NCS})$ . Similarly, **1**, **4**, and **7** showed a strong band at  $\sim 845 \text{ cm}^{-1}$  due to  $\nu(\text{PF}_6^-)$  and **2**, **5**, and **8** exhibited a broad band at  $\sim 1065 \text{ cm}^{-1}$  due to  $\nu(\text{BF}_4^-)$ , indicating the presence of  $\text{PF}_6^-$  and  $\text{BF}_4^-$ , respectively. The IR spectra of **3**, **6**, and **9** exhibited a broad band at  $\sim 1078 \text{ cm}^{-1}$  due to  $\nu_{\text{assy}}(\text{Cl-O})$  and a weak band at  $\sim 623 \text{ cm}^{-1}$  due to  $\delta(\text{O-Cl-O})$ , confirming the presence of perchlorate outside the coordination sphere in the complexes.

The complexes exhibit several absorptions in  $\text{CH}_3\text{CN}$  from 200 to 900 nm. The high intensity bands at  $\sim 245$  and  $\sim 325 \text{ nm}$  are due to intraligand  $n\text{-}\pi^*/\pi\text{-}\pi^*$  transitions. The three absorptions at  $\sim 725$ ,  $\sim 580$ , and  $\sim 490 \text{ nm}$  are due to d-d transition or ligand field transitions. Such transitions are generally observed for high spin cobalt(II) complexes with trigonal bipyramidal geometry [40]. Room temperature powder sample magnetic moment of the complexes are 4.16–4.32 BM, indicating three unpaired electrons in the high spin cobalt(II) ion. Magnetic moments for cobalt(II) complexes with tripodal ligand fall in the range of 4.4–4.7 BM [29].

### 3.3. Description of crystal structures

**3.3.1.  $[\text{Co}(\text{N}_3)(\text{dbdmp})]\text{PF}_6$  (**1**) and  $[\text{Co}(\text{N}_3)(\text{dbdmp})]\text{ClO}_4$  (**3**).** An ORTEP view with atom numbering scheme of the cationic part of **1** and **3** are shown in figures 1 and 2. Selected bond lengths and angles relevant to the coordination sphere are listed in table 2. Complex **1** crystallizes in the monoclinic chiral space group  $C2$  which consists of two crystallographically independent  $[\text{Co}(\text{N}_3)(\text{dbdmp})]^+$  complex cations and two  $\text{PF}_6^-$  anions in the asymmetric unit, whereas **3** crystallizes in the monoclinic space group  $P2_1/c$  which consists of  $[\text{Co}(\text{N}_3)(\text{dbdmp})]^+$  and  $\text{ClO}_4^-$ . The cobalt(II) adopts slightly distorted trigonal bipyramidal coordination geometry with a  $\text{CoN}_5$  coordination environment in both complexes, which is revealed by the magnitude of the trigonality index ( $\tau = 0.96$  and  $0.85$  for **1** and **3**,

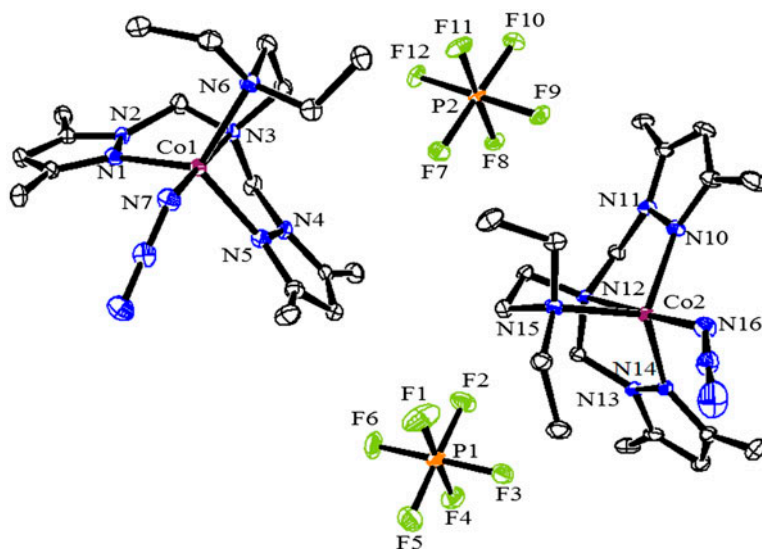


Figure 1. ORTEP diagram of **1** with atom numbering scheme (30% probability factor for the thermal ellipsoids, hydrogens were omitted for clarity).

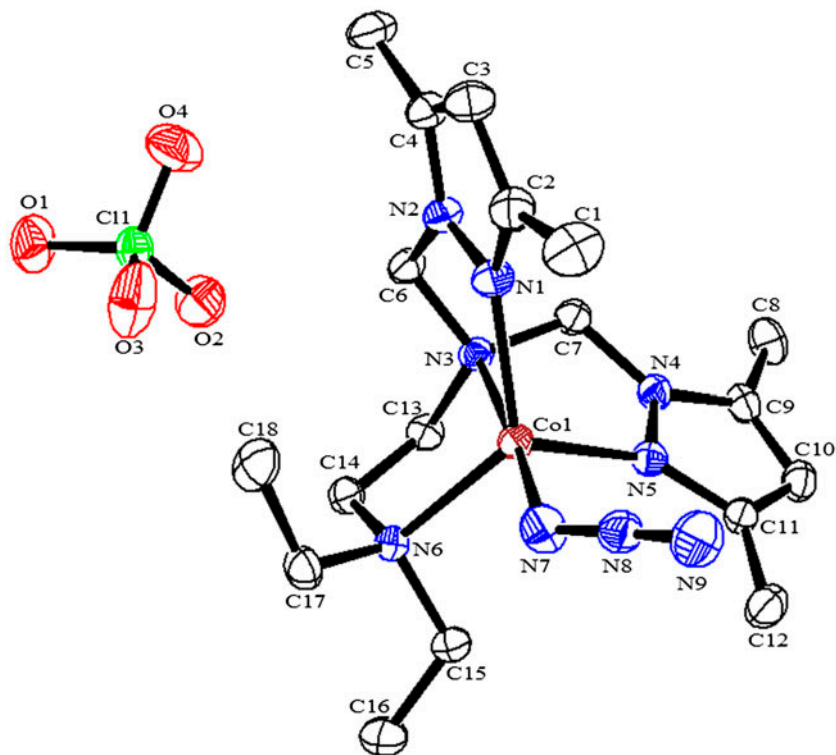


Figure 2. ORTEP diagram depicting **3** with atom numbering scheme (30% probability factor for the thermal ellipsoids, hydrogens were omitted for clarity).

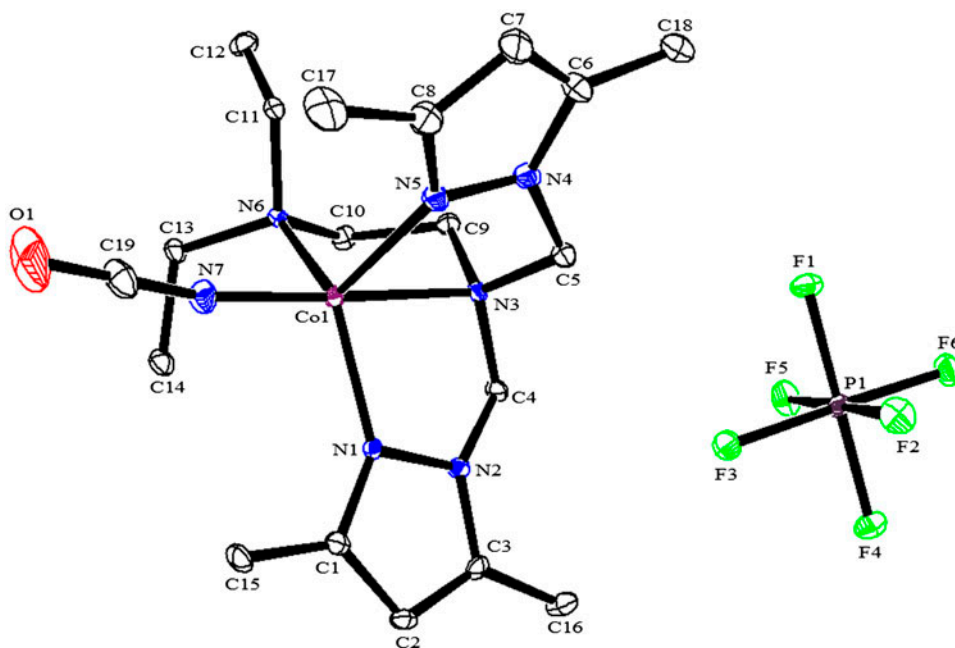


Figure 3. ORTEP diagram depicting **4** with atom numbering scheme (30% probability factor for the thermal ellipsoids, hydrogens were omitted for clarity).

respectively) [41]. Four nitrogens [N(1), N(3), N(5), and N(6)] of the tetradentate ligand in combination with one nitrogen [N(7)] of azide completed trigonal bipyramidal geometry of the cobalt center. The equatorial positions are occupied by three nitrogens of the tetradentate ligand, i.e., two nitrogens [N(1), N(5)] from two pyrazole rings and one nitrogen [N(6)] from tertiary amine, while another tertiary amine [N(3)] of dbdmp and nitrogen from azide [N(7)] are placed at axial positions. The equatorial bond distances of Co(1)–N(1), Co(1)–N(5), and Co(1)–N(6) are 2.036(3)–2.124(4) Å, nearly equal, but the two axial distances of Co(1)–N(3) (2.256(3) Å for **1** and 2.2435(19) Å for **2**) are longer than that of Co(1)–N(7) (2.001(3) Å for **1** and 1.999(2) Å for **2**). The cobalt–tertiary amine bond lengths are most elongated and comparable to reported cobalt(II) complex with dbdmp (2.252(4) Å) [42] and cobalt(II) chloride complex with tripodal tris(2-pyridylmethyl)amine (TPA) (2.2841(18) Å) [36]. The equatorial bond angles are 109.83(8)°–119.29(12)°, whereas axial bond angle N(3)–Co(1)–N(7) is 177.25(13)° and 176.15(9)° for **1** and **3**, respectively.

**3.3.2. [Co(NCO)(dbdmp)]PF<sub>6</sub> (**4**) and [Co(NCO)(dbdmp)]ClO<sub>4</sub> (**6**).** An ORTEP view with atom numbering scheme of **4** and **6** are shown in figures 3 and 4, respectively. Complex **4** crystallizes in the orthorhombic chiral space group  $P2_12_12_1$ , whereas **6** crystallizes in the monoclinic space group  $P2_1/c$ . For the two complexes, cobalt(II) has a distorted trigonal bipyramidal geometry ( $\tau = 0.99$  for **4** and 0.89 for **6**) with CoN<sub>5</sub> coordination environment, respectively. In **4** and **6**, four nitrogens [N(1), N(3), N(5) and N(6)] of the tetradentate dbdmp in combination with one nitrogen [N(7)] of NCO<sup>−</sup> completed trigonal bipyramidal coordination of the metal ion. The equatorial positions are occupied by three nitrogens of

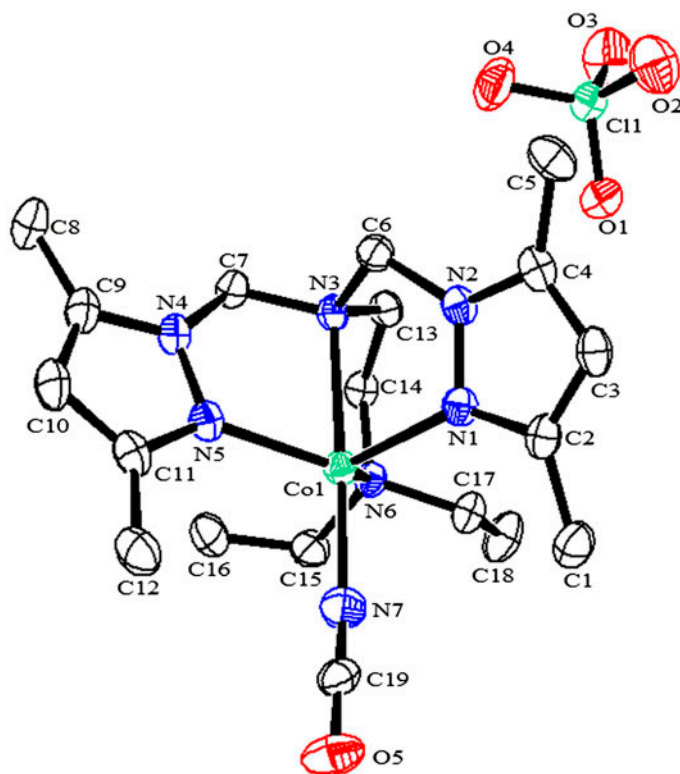


Figure 4. ORTEP diagram depicting **6** with atom numbering scheme (30% probability factor for the thermal ellipsoids, hydrogens were omitted for clarity).

the tetradentate ligand, i.e., N(1) and N(5) of the pyrazole rings and N(6) of the tertiary amine, while another tertiary amine N(3) of ligand and N(7) of the  $\text{NCO}^-$  are placed at axial positions. The equatorial bond distances of **4**, Co(1)–N(1), Co(1)–N(5), and Co(1)–N(6), are 2.040(3)–2.108(3) Å and are nearly equal but the axial bond distance of Co(1)–N(3) (2.330(3) Å) is longer than Co(1)–N(7) (1.950(4) Å). In **6**, the axial bond distance of Co(1)–N(3) (2.255(4) Å) is shorter than Co(1)–N(3) (2.329(3) Å) of **4**, whereas the Co(1)–N(7) (1.997(5) Å) bond distance of **6** is nearly equal to the Co(1)–N(7) (1.950(4) Å) distance of **4**. The equatorial bond angles are 109.39(14)°–124.76(8)°, whereas the axial bond angle N(3)–Co(1)–N(7) is 178.41(15)° for **4** and N(3)–Co(1)–N(7) is 178.13(9)° for **6**.

**3.3.3. [Co(NCS)(dbdmp)]ClO<sub>4</sub> (**9**).** The complex crystallizes in the monoclinic system with space group  $P2_1/c$ . The ORTEP diagram of **9** along with the atom labeling scheme is shown in figure 5. The cobalt(II) center adopts a distorted trigonal bipyramidal coordination geometry ( $\tau = 0.88$ ) with  $\text{CoN}_5$  coordination. Four nitrogens [N(1), N(3), N(5), and N(6)] of the tetradentate ligand in combination with N(7) of thiocyanate complete trigonal bipyramidal coordination of the cobalt(II). The equatorial positions are occupied by three nitrogens of the tetradentate ligand, i.e., pyrazole ring nitrogens [N(1), N(5)] and tertiary amine [N(6)], while another tertiary amine [N(3)] and thiocyanate N(7) are at axial positions. The equatorial bond distances of Co(1)–N(1), Co(1)–N(5), and Co(1)–N(6) are 2.057

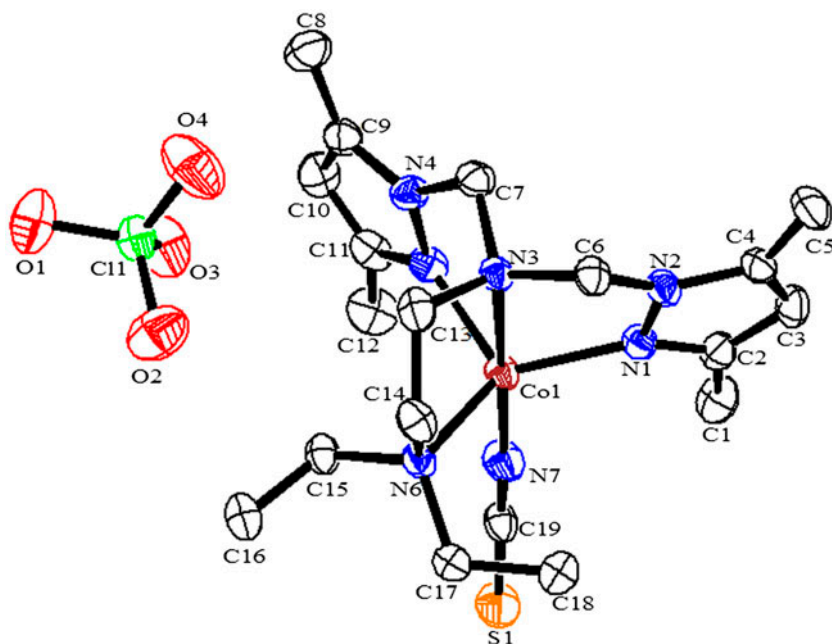


Figure 5. ORTEP diagram depicting **9** with atom numbering scheme (30% probability factor for the thermal ellipsoids, hydrogens were omitted for clarity).

(3)–2.132(3) Å, but the axial bond distance of Co(1)–N(3) (2.245(3) Å) is longer than Co(1)–N(7) (1.981(4) Å). The equatorial bond angles are 111.94(12)°–122.76(11)°, whereas axial bond angle N(3)–Co(1)–N(7) is 175.78(13)°.

### 3.4. DNA and BSA binding study

**3.4.1. Electronic absorption titration with CT-DNA.** Transition metal complexes can bind to DNA via both covalent and/or non-covalent interactions. In the case of covalent binding, the labile ligand of the complexes can be replaced by a nitrogen base of DNA such as guanine N7, while the non-covalent DNA interactions include intercalative, electrostatic, and groove (surface) binding of metal complexes outside of the DNA helix, along the major or minor groove [10, 43]. Hyperchromism and hypochromism are spectral changes of metal complex association with the DNA helix. Hyperchromism means the breakage of the secondary structure of DNA and hypochromism means the DNA binding mode of complex is electrostatic or intercalation which can stabilize the DNA duplex, while the existence of a red shift is indicative of stabilization of the DNA duplex [44]. Complex binding with DNA usually results in hypochromism and red shift arising from strong stacking interaction between complex and DNA [45–49].

The binding ability of **1**, **4**, and **7** with CT-DNA are studied by measuring absorption spectroscopy. The absorption spectra of the cobalt(II) complexes are characterized by intense  $\pi$ - $\pi^*$  ligand-based transitions in the UV and d-d transitions in the visible region. The absorption spectra of **1**, **4**, and **7** in the absence and presence of CT-DNA are presented in figure 6 (a), (b), and (c), respectively. The absorption bands of d-d transitions are

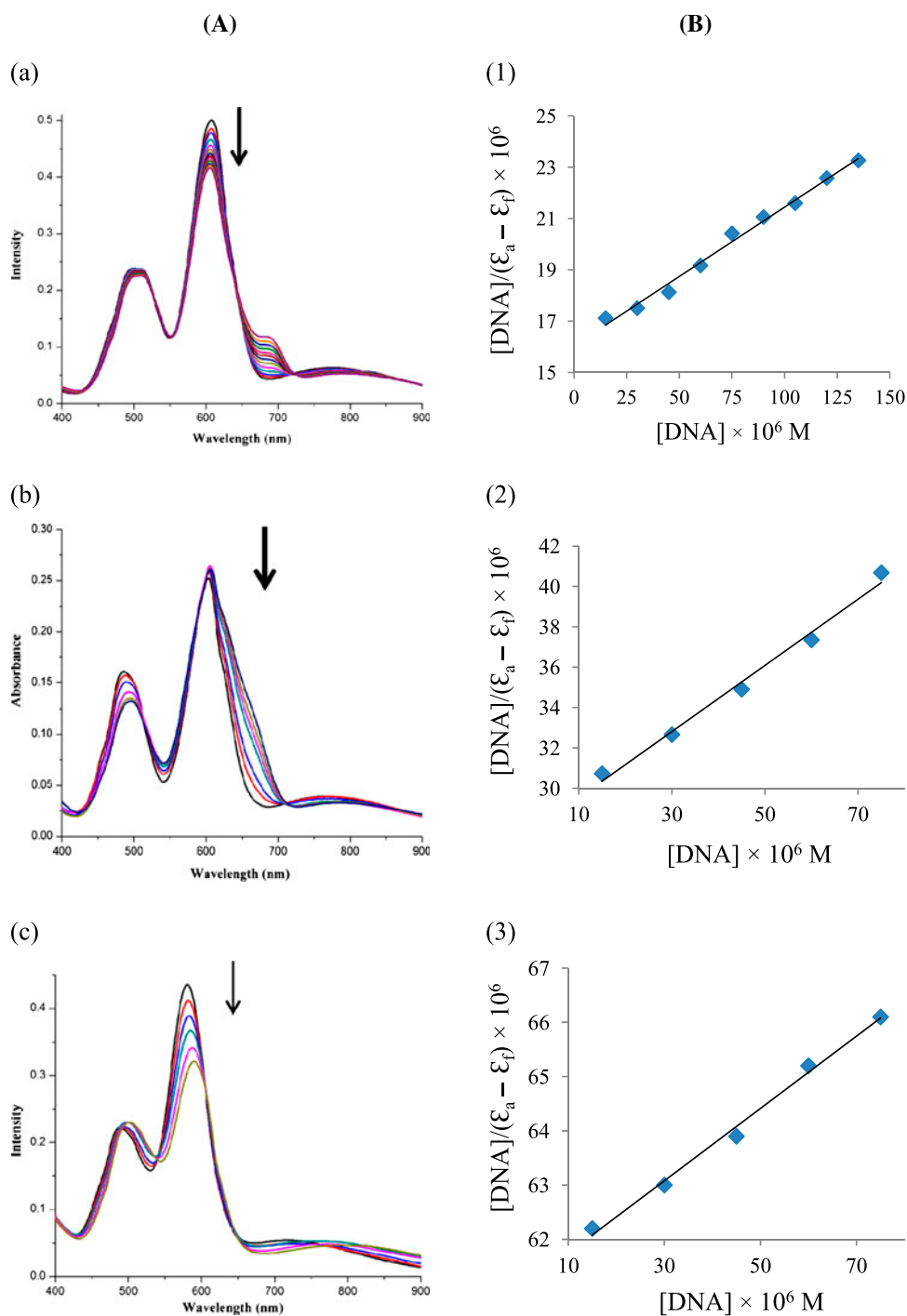


Figure 6. (A) Absorption spectra of **1**, **4**, and **7** ( $1 \times 10^{-3}$  M) in the absence and presence of increasing amounts of CT-DNA (0–200  $\mu$ M) at 25  $^{\circ}$ C in Tris-HCl/NaCl buffer (pH 7.2). Arrow shows the absorbance changing upon increasing DNA concentrations. (B) Least squares fit of  $[\text{DNA}]/(\epsilon_a - \epsilon_f)$  vs.  $[\text{DNA}]$  for **1**, **4**, and **7**.

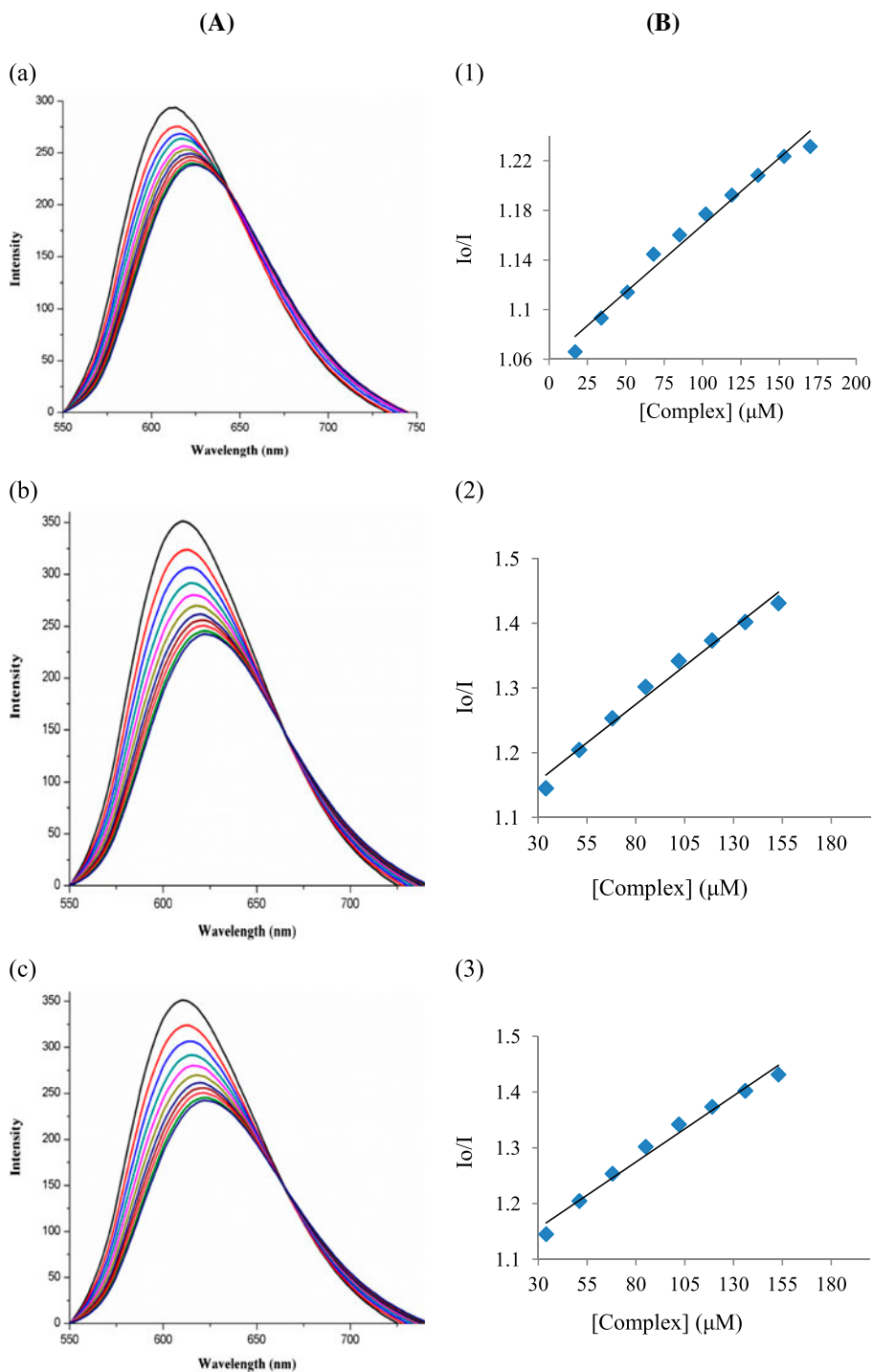
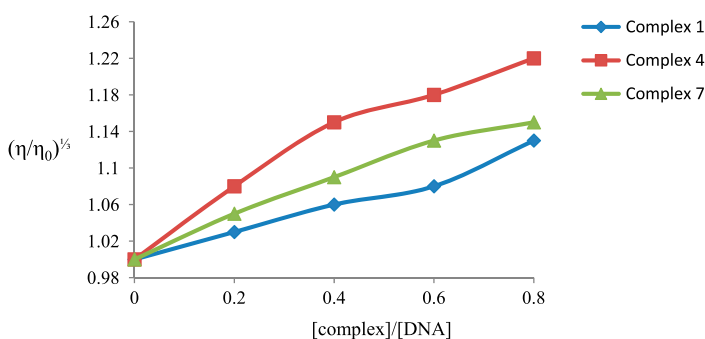


Figure 7 (A) Fluorescence quenching spectra of **1**, **4**, and **7** ( $\lambda_{\text{ex}} = 510 \text{ nm}$ ) by addition of increasing amount of complexes (0–160  $\mu\text{M}$ ) to EB-bound CT-DNA. (B) The plot of  $I_0/I$  vs. [complex] for **1**, **4**, and **7**.



Table 3. CT-DNA binding parameters of complexes.

Complex	$K_b$ ( $M^{-1}$ )	$K_{sv}$ ( $M^{-1}$ )	$K_{sv}$ (BSA) ( $M^{-1}$ )
$[Co(N_3)(dbdmp)]PF_6$ ( <b>1</b> )	$2.7 (\pm 0.02) \times 10^5$	$1.1 (\pm 0.06) \times 10^3$	$2.8 (\pm 0.01) \times 10^3$
$[Co(NCO)(dbdmp)]PF_6$ ( <b>4</b> )	$3.93 (\pm 0.03) \times 10^5$	$2.4 (\pm 0.01) \times 10^3$	$3.0 (\pm 0.09) \times 10^3$
$[Co(NCS)(dbdmp)]PF_6$ ( <b>7</b> )	$3.4 (\pm 0.01) \times 10^5$	$1.3 (\pm 0.07) \times 10^3$	$2.7 (\pm 0.06) \times 10^3$

Figure 8. Effects of increasing amounts of **1**, **4**, and **7** on the relative viscosities of CT-DNA at  $30 \pm 0.01$  °C,  $[DNA] = 0.5$  mM.

observed for **1** at 502, 607, and 781 nm. The band centered at 606 nm exhibits hypochromism by a small blue shift. Such spectral changes in d–d transitions suggest that there are some interactions like surface binding between the cobalt(II) complex and DNA [50–52]. Formation of a new band at 690 nm with a hyperchromic change suggests that the complex could uncoil the helix structure of DNA and made more bases embedding in DNA exposed [53]. Two isobestic points were observed at 642 and 722 nm which indicate the direct formation of a new complex with double-helical CT-DNA and Co(II) [51].

The absorption bands of d–d transitions are observed at 489, 599, and 765 nm for **4** and at 489, 580, and 723 nm for **7**. When **4** and **7** are titrated with CT-DNA, hypochromism, and slight blue shift is observed in the UV region (see supplementary material), whereas red-shift is observed in d–d bands. In addition, three isobestic points were observed at 423, 514, and 710 nm for **4** and 495, 536, and 794 nm for **7**, which indicates the direct formation of a new complex with double-helical CT-DNA [52]. The observed hypochromism and red-shift suggest stabilization of the DNA duplex [44]. Such spectral changes in visible region suggest surface binding or non-covalent binding between the cobalt(II) complex and DNA [50, 52]. Recently, we reported DNA binding of copper(II) complexes with the same ligand but no such isobestic point was observed in the UV or visible region. This also suggests new complex formation with CT-DNA and cobalt(II) complex [18].

In order to compare quantitative binding strength of the complexes, the intrinsic binding constants  $K$  of the complexes to CT-DNA were determined by monitoring the changes of absorbance at 607 nm (for **1**), 485 nm (for **4**), and 580 nm (for **7**) with increasing concentration of DNA. The intrinsic binding constants  $K_b$  of **1**, **4**, and **7** are  $2.7 (\pm 0.02) \times 10^5$ ,  $3.93 (\pm 0.03) \times 10^5$ , and  $3.4 (\pm 0.01) \times 10^5$ , respectively. The exact mode of binding cannot be proposed by UV spectroscopic titration studies. In most cases, the existence of hypochromism

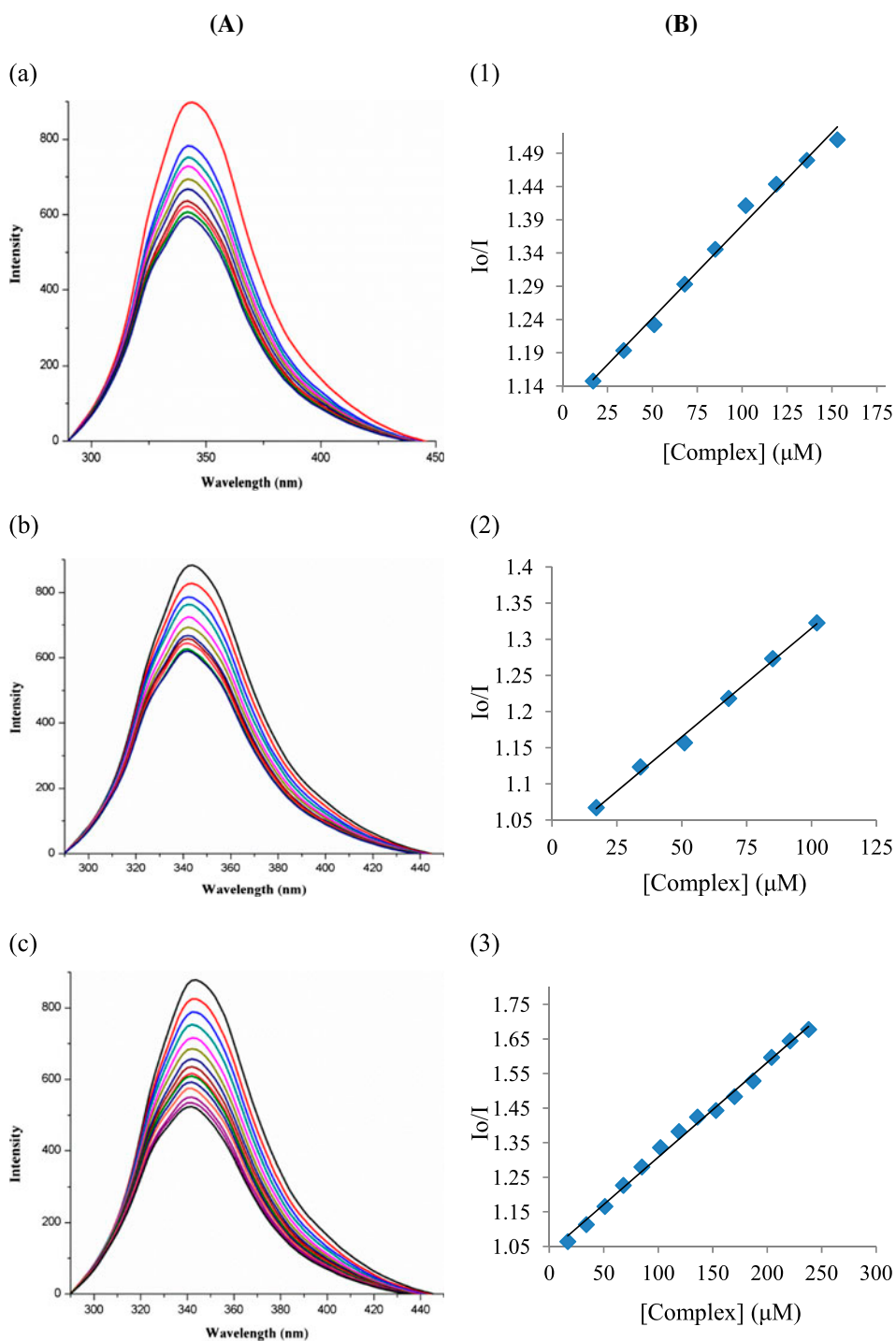


Figure 9. (a) Fluorescence quenching spectra of BSA (3 mL, 50  $\mu\text{M}$ ) with increasing amount of **1**, **4**, and **7** (0–300  $\mu\text{M}$ ) in Tris-HCl/NaCl buffer (pH 7.2) at 25  $^{\circ}\text{C}$ . (b) Stern–Volmer plot for the quenching of BSA fluorescence by **1**, **4**, and **7**.

for all complexes could be considered as evidence that the binding of the complexes involving intercalation between the base pairs of CT-DNA cannot be ruled out [54–59].

**3.4.2. Fluorescence spectral studies.** As the present complexes are non-fluorescent at room temperature in solution or in the presence of DNA, competitive ethidium bromide binding experiments were carried out to gain support for the extent of binding with CT-DNA. The emission spectra of EB bound to DNA in the absence and presence of each complex were recorded in the Tris buffer for  $[EB] = 20 \mu\text{M}$  and  $[DNA] = 30 \mu\text{M}$  for increasing amounts of each complex. The fluorescence quenching curves of EB bound to DNA by **1**, **4**, and **7** are shown in figure 7 (a), (b), and (c) and the reduction in the intensity of the emission band suggests that the complexes compete with EB and strongly bind with DNA through intercalation. The Stern–Volmer plots of DNA-EB [figure 7 (1), (2), and (3)] illustrate that the quenching of EB-DNA fluorescence by the compounds are in agreement ( $R = 0.9$ ) with the linear Stern–Volmer equation [54–56, 60], also suggesting strong binding of the complexes with DNA. The Stern–Volmer quenching constant values (table 3) are less than the binding constant of the classical intercalators and metallointercalators ( $10^7 \text{ M}^{-1}$ ) [61].

**3.4.3. Viscosity measurements.** Hydrodynamic methods (*i.e.*, viscosity and sedimentation) that are sensitive to the changes in the effective length of DNA molecules are crucial to find the nature of binding of metal complexes to the DNA. This study was regarded as the least ambiguous and the most critical test of binding mode in solution state in the absence of crystallographic structural data [62–64]. Under the appropriate conditions, intercalation results in lengthening the DNA helix as base pairs separated to accommodate the binding ligand, leading to increase of DNA viscosity. Partial or non-classical intercalation of ligand could bend (or kink) the DNA helix and reduce its effective length concomitantly and its viscosity [65, 66]. The changes in the relative viscosity of rod-like CT-DNA in the presence of increasing amount of **1**, **4**, and **7** are shown in figure 8. The viscosity of DNA increases steadily with increasing concentration of the complexes. The experimental results suggest that complexes bind to DNA through a classical intercalation mode. However, this increase is relatively less as compared to classical intercalators EB. So, we can conclude that **1**, **4**, and **7** strongly interact via surface binding or non-covalent binding, which is supported by UV spectroscopic titration studies.

**3.4.4. Fluorescence quenching of BSA by complexes.** Serum albumin is the most abundant protein in plasma which is involved in transport of metal ions and metal complexes with drugs through the blood stream. Binding to these proteins may lead to loss or enhancement of biological properties of the original drug or provide paths for drug transportation [10]. BSA is the most extensively studied serum albumin because of its structural homology with human serum albumin. Binding of transition metal complexes to BSA have also been interesting in chemistry, life sciences, and clinical medicine as it greatly influences absorption, drug transport, storage, metabolism, and excretion properties of typical drugs in vertebrates [67].

BSA solution exhibits an intense fluorescence emission band with a peak at 343 nm due to the tryptophan residue when excited at 290 nm [23]. The fluorescence emission spectra of

BSA in the presence of **1**, **4**, and **7** were studied with increasing the concentrations of the complexes and shown in figure 9 (a), (b), and (c). The changes and quenching of fluorescence emission spectra upon addition of **1**, **4**, and **7** may be due to the changes in protein conformation, subunit association, substrate binding, or denaturation because of the complex binding [68]. The fluorescence quenching is described by the Stern–Volmer equation:  $I_0/I = 1 + K_{sv}[Q]$ , where  $I_0$  and  $I$  are the emission intensities in the absence and presence of the complexes, respectively,  $K_{sv}$  is the dynamic quenching constant, and  $[Q]$  is the total concentration of complexes. The calculated values of  $K_{sv}$  for **1**, **4**, and **7** are  $2.8 (\pm 0.01) \times 10^3$ ,  $3.0 (\pm 0.09) \times 10^3$ , and  $2.7 (\pm 0.06) \times 10^3 \text{ M}^{-1}$ , respectively, which are obtained by the slope of the Stern–Volmer plot indicating the good binding propensity. These binding constant values are lower than that of the avidin–ligands binding affinity ( $K_{\text{avidin-ligands}} \cong 10^{15} \text{ M}^{-1}$ ) which is among the highest observed so far [69]. In the comparison of the complexes (table 3), **4** shows higher binding affinity for BSA than **1** and **7**. So the interaction of **1**, **4**, and **7** with BSA may provide useful information for potential applications.

#### 4. Conclusion

Mononuclear five-coordinate cobalt(II) complexes,  $[\text{Co}(\text{X})(\text{dbdmp})]\text{Y}$ , where  $\text{dbdmp} = N,N$ -diethyl- $N',N'$ -bis((3,5-dimethyl-*1H*-pyrazol-1-yl)methyl)ethane-1,2-diamine,  $\text{X} = \text{N}_3^-/\text{NCS}^-/\text{NCO}^-$  and  $\text{Y} = \text{ClO}_4^-/\text{PF}_6^-/\text{BF}_4^-$ , have been synthesized and characterized. Structural studies show all the complexes have distorted trigonal bipyramidal geometry and  $\text{N}_3^-$  and  $\text{NCO}^-$  containing cobalt(II) complexes with  $\text{PF}_6^-$  counter ion have chiral space group, whereas complexes with  $\text{ClO}_4^-$  have non-chiral space groups. CT-DNA bindings of the cobalt(II) complexes were investigated by absorption, fluorescence spectroscopy, and viscosity measurements and BSA binding study by fluorescence spectroscopy. The results indicate that the complexes can interact strongly with DNA base pair and protein.

#### Supplementary material

CCDC 890815, 949199, 1415315, 991574, and 996282 contain the supplementary crystallographic data for **1**, **3**, **4**, **6**, and **9**. This data can be obtained free of charge via <http://www.ccdc.cam.ac.uk/conts/retrieving.html>, or from the Cambridge Crystallographic Data Center, 12 Union Road, Cambridge CB12 1EW, UK (Fax:+44-1223-336 033; E-mail: [deposit@ccdc.cam.ac.uk](mailto:deposit@ccdc.cam.ac.uk)).

#### Acknowledgements

Financial support from UGC in the form of major research project (F.No. 39-720/2010(SR)) is gratefully acknowledged. A. Solanki thanks UGC for BSR fellowship. We thank Dr P. Paul and Dr E. Suresh of Central Salt and Marine Chemicals Research Institute, Bhavnagar, for spectroscopy and X-ray studies, IIT Roorkey and DST PURSE program, Department of Chemistry, the M.S. University of Baroda, Vadodara, for single-crystal X-ray

diffraction study. We thank Mr Hemant Mande of M.S. University of Baroda for helping in crystallography. We also thank one of the reviewers for suggestions on crystallography.

### Disclosure statement

No potential conflict of interest was reported by the authors.

### Funding

This work was financially supported by the University Grants Commission [F.No. 39-720/2010(SR)].

### Supplemental data

Supplemental data for this article can be accessed [<http://dx.doi.org/10.1080/00958972.2015.1085515>].

### References

- [1] A.M. Pyle, E.C. Long, J.K. Barton. *J. Am. Chem. Soc.*, **111**, 4520 (1989).
- [2] A. Sitlani, E.C. Long, A.M. Pyle, J.K. Barton. *J. Am. Chem. Soc.*, **114**, 2303 (1992).
- [3] L. Jin, P. Yang. *Polyhedron*, **16**, 3395 (1997).
- [4] Y.-M. Song, X.-I. Lu, M.-I. Yang, X.-R. Zheng. *Transition Met. Chem.*, **30**, 499 (2005).
- [5] X.L. Wang, H. Chao, H. Li, X.L. Hong, Y.J. Liu, L.F. Tan, L.N. Ji. *J. Inorg. Biochem.*, **98**, 1143 (2004).
- [6] S. Ramakrishnan, E. Suresh, A. Riyasdeen, M.A. Akbarsha, M. Palaniandavar. *Dalton Trans.*, **40**, 3524 (2011).
- [7] S. Budagumpi, N.V. Kulkarni, G.S. Kurdekar, M.P. Sathisha, V.K. Revankar. *Eur. J. Med. Chem.*, **45**, 455 (2010).
- [8] M.N. Patel, M.R. Chhasatia, D.S. Gandhi. *Bioorg. Med. Chem. Lett.*, **19**, 2870 (2009).
- [9] E.K. Efthimiadou, A. Karaliota, G. Psomas. *Bioorg. Med. Chem. Lett.*, **18**, 4033 (2008).
- [10] F. Dimiza, A.N. Papadopoulos, V. Tangoulis, V. Psycharis, C.P. Raptopoulou, D.P. Kessissoglou, G. Psomas. *Dalton Trans.*, **39**, 4517 (2010).
- [11] F. Zhang, Q.Y. Lin, W.D. Liu, P.P. Wang, W.J. Song, B.-W. Zheng. *J. Coord. Chem.*, **66**, 2297 (2013).
- [12] X. Fan, J. Dong, R. Min, Y. Chen, X. Yi, J. Zhou, S. Zhang. *J. Coord. Chem.*, **66**, 4268 (2013).
- [13] B. Li, W. Liu, J. Shao, C.L. Xue, C.Z. Xie, Y. Ouyang, J.Y. Xu. *J. Coord. Chem.*, **66**, 2465 (2013).
- [14] T.-F. Miao, S. Li, J. Li, K.-C. Zheng. *J. Inorg. Biochem.*, **109**, 16 (2012).
- [15] B. Peng, H. Chao, B. Sun, H. Li, F. Gao, L.-N. Ji. *J. Inorg. Biochem.*, **101**, 404 (2007).
- [16] A. Panja. *Polyhedron*, **43**, 22 (2012).
- [17] R.S. Kumar, S. Arunachalam. *Polyhedron*, **25**, 3117 (2006).
- [18] A. Solanki, S.B. Kumar, A.A. Doshi, C. Ratna Prabha. *Polyhedron*, **63**, 147 (2013).
- [19] M.F. Reichmann, S.A. Rice, C.A. Thomas, P. Doty. *J. Am. Chem. Soc.*, **76**, 3047 (1954).
- [20] O. Gia, S.M. Marciani Magno, H. Gonzalez-Diaz, E. Quezada, L. Santana, E. Uriarte, L. Dalla Via. *Bioorg. Med. Chem.*, **13**, 809 (2005).
- [21] A.M. Pyle, J.P. Rehmann, R. Meshoyrer, C.V. Kumar, N.J. Turro, J.K. Barton. *J. Am. Chem. Soc.*, **111**, 3051 (1989).
- [22] J.R. Lakowicz, G. Webber. *Biochemistry*, **12**, 4164 (1973).
- [23] J.R. Lakowicz. *Principles of Fluorescence Spectroscopy*, 2nd Edn., Plenum Press, New York (1999).
- [24] G.M. Sheldrick. *SAINTE*, 5.1 Edn., Siemens Industrial Automation Inc., Madison, WI (1995).
- [25] Agilent. *CrysAlis PRO*, Agilent Technologies UK Ltd., Yarnton, England (2011).
- [26] G.M. Sheldrick. *SADABS, Empirical Absorption Correction Program*, University of Gottingen, Gottingen, Germany (1997).
- [27] G.M. Sheldrick. *SHELXTL Reference Manual (Version 5.1)*, Bruker AXS, Madison, WI (1997).
- [28] G.M. Sheldrick. *SHELXL-97: Program for Crystal Structure Refinement*, University of Gottingen, Gottingen (1997).
- [29] S. Sabiah, B. Varghese, N.N. Murthy. *Dalton Trans.*, 9770 (2009).
- [30] J.R. Cubanski, S.A. Cameron, J.D. Crowley, A.G. Blackman. *Dalton Trans.*, **42**, 2174 (2013).
- [31] S.S. Massoud, F.R. Louka, Y.K. Obaid, R. Vicente, J. Ribas, R.C. Fischer, F.A. Mautner. *Dalton Trans.*, **42**, 3968 (2013).

- [32] F.A. Saad, N.J. Buurma, A.J. Amoroso, J.C. Knight, B.M. Kariuki. *Dalton Trans.*, **41**, 4608 (2012).
- [33] S.S. Massoud, L.L. Quan, K. Gatterer, J.H. Albering, R.C. Fischer, F.A. Mautner. *Polyhedron*, **31**, 601 (2012).
- [34] S.S. Massoud, K.T. Broussard, F.A. Mautner, R. Vicente, M.K. Saha, I. Bernal. *Inorg. Chim. Acta*, **361**, 123 (2008).
- [35] S.B. Kumar, Z. Mahendrasinh, S. Ankita, R. Mohammedayaz, P. Pragna, E. Suresh. *Polyhedron*, **36**, 15 (2012).
- [36] C.J. Davies, G.A. Solan, J. Fawcett. *Polyhedron*, **23**, 3105 (2004).
- [37] A. Garoufis, S. Kasselouri, C.P. Raptopoulou. *Inorg. Chem. Commun.*, **3**, 251 (2003).
- [38] T.M. Kooistra, K.F.W. Hekking, Q. Knijnenburg, B. de Bruin, P.H.M. Budzelaar, R. de Gelder, J.M.M. Smits, A.W. Gal. *Eur. J. Inorg. Chem.*, **4**, 648 (2003).
- [39] K. Nakamoto. *Infrared and Raman Spectra of Inorganic and Coordination Compounds*, Wiley-Interscience, New York (1986).
- [40] A. Garoufis, S. Kasselouri, C.P. Raptopoulou. *Inorg. Chem. Commun.*, **3**, 251 (2000).
- [41] A.W. Addison, T.N. Rao, J. Reedijk, J. van Rijn, G.C. Verschoor. *J. Chem. Soc., Dalton Trans.*, 1349 (1984).
- [42] A. Solanki, S.B. Kumar. *Polyhedron*, **81**, 323 (2014).
- [43] Q. Zhang, J. Liu, H. Chao, G. Xue, L. Ji. *J. Inorg. Biochem.*, **83**, 49 (2001).
- [44] E.C. Long, J.K. Barton. *Acc. Chem. Res.*, **23**, 271 (1990).
- [45] C. Hiort, P. Lincoln, B. Norden. *J. Am. Chem. Soc.*, **115**, 3448 (1993).
- [46] L. Fin, P. Yang. *J. Inorg. Biochem.*, **68**, 79 (1997).
- [47] Mudasir, K. Wijaya, D.H. Tjahjono, N. Yoshioka, H. Inoue. *Z. Naturforsch.*, **59b**, 310 (2004).
- [48] M. Navarro, E.J. Cisneros-Fajardo, M. Fernandez-Mestre, D. Arrièche, E. Marchan. *J. Biol. Inorg. Chem.*, **8**, 401 (2003).
- [49] R.B. Nair, E.S. Teng, S.L. Kirkland, C.J. Murphy. *Inorg. Chem.*, **37**, 139 (1998).
- [50] P.T. Selvi, H. Stoeckli-Evans, M. Palaniandavar. *J. Inorg. Biochem.*, **99**, 2110 (2005).
- [51] A. Ray, B.K. Koley Seth, U. Pal, S. Basu. *Spectrochim. Acta, Part A*, **92**, 164 (2012).
- [52] K. Ghosh, P. Kumar, N. Tyagi. *Inorg. Chim. Acta*, **375**, 77 (2011).
- [53] G. Pratviel, J. Bernadou, B. Meunier. *Adv. Inorg. Chem.*, **45**, 251 (1998).
- [54] K.C. Skyrianou, F. Perdih, I. Turel, D.P. Kessissoglou, G. Psomas. *J. Inorg. Biochem.*, **104**, 161 (2010).
- [55] K.C. Skyrianou, V. Psycharis, C.P. Raptopoulou, D.P. Kessissoglou, G. Psomas. *J. Inorg. Biochem.*, **105**, 63 (2011).
- [56] A. Tarushi, C.P. Raptopoulou, V. Psycharis, A. Terzis, G. Psomas, D.P. Kessissoglou. *Bioorg. Med. Chem.*, **18**, 2678 (2010).
- [57] G. Psomas, A. Tarushi, E.K. Efthimiadou, Y. Sanakis, C.P. Raptopoulou, N. Katsaros. *J. Inorg. Biochem.*, **100**, 1764 (2006).
- [58] A. Tarushi, G. Psomas, C.P. Raptopoulou, D.P. Kessissoglou. *J. Inorg. Biochem.*, **103**, 898 (2009).
- [59] B.C. Baguley, M. Le Bret. *Biochemistry*, **23**, 937 (1984).
- [60] G. Psomas. *J. Inorg. Biochem.*, **102**, 1798 (2008).
- [61] M. Cory, D.D. McKee, J. Kagan, D.W. Henry, J.A. Miller. *J. Am. Chem. Soc.*, **107**, 2528 (1985).
- [62] S. Zhang, Y. Zhu, C. Tu, H. Wei, Z. Yang, L. Lin, J. Ding, J. Zhang, Z. Guo. *J. Inorg. Biochem.*, **98**, 2099 (2004).
- [63] V.A. Izumrudov, M.V. Zhiryakova, A.A. Goulko. *Langmuir*, **18**, 10348 (2002).
- [64] J. Liu, T. Zhang, T. Lu, L. Qu, H. Zhou, Q. Zhang, L. Ji. *J. Inorg. Biochem.*, **91**, 269 (2002).
- [65] S. Satyanarayana, J.C. Dabrowiak, J.B. Chaires. *Biochemistry*, **31**, 9319 (1992).
- [66] S. Satyanarayana, J.C. Dabrowiak, J.B. Chaires. *Biochemistry*, **32**, 2573 (1993).
- [67] Y.Z. Zhang, H.R. Li, J. Dai, W.J. Chen, J. Zhang, Y. Liu. *Biol. Trace Elem. Res.*, **135**, 136 (2010).
- [68] Y. Wang, H. Zhang, G. Zhang, W. Tao, S. Tang. *J. Luminesc.*, **126**, 211 (2007).
- [69] E. Chalkidou, F. Perdih, I. Turel, D.P. Kessissoglou, G. Psomas. *J. Inorg. Biochem.*, **113**, 55 (2012).